Robotica (2015) volume 33, pp. 87–105. © Cambridge University Press 2014
doi:10.1017/S0263574714000046

Saturated output feedback control of uncertain nonholonomic wheeled mobile robots

Khoshnam Shojaei*

Department of Electrical Engineering, Najafabad Branch, Islamic Azad University, Najafabad, Iran

(Accepted December 22, 2013. First published online: January 31, 2014)

SUMMARY

Many research works on the control of nonholonomic wheeled mobile robots (WMRs) do not consider the actuator saturation problem and the absence of velocity sensors in practice. The actuator saturation deteriorates the tracking performance of the controller, and the use of velocity sensors increases the cost and weight of WMR systems. This paper simultaneously addresses these problems by designing a saturated output feedback controller for uncertain nonholonomic WMRs. First, a second-order input–output model of nonholonomic WMRs is developed by defining a suitable set of output equations. Then a saturated adaptive robust tracking controller is proposed without velocity measurements. For this purpose, a nonlinear saturated observer is used to estimate robot velocities. The risk of actuator saturation is effectively reduced by utilizing saturation functions in the design of the observer–controller scheme. Semi-global uniform ultimate boundedness of error signals is guarantied by the Lyapunov stability analyses. Finally, simulation results are provided to show the effectiveness of the proposed controller. Compared with one recent work of the author, a comparative study is also presented to illustrate that the proposed saturated controller is more effective when WMR actuators are subjected to saturation.

KEYWORDS: Actuator saturation; Adaptive control; Nonholonomic robots; Output feedback control; Trajectory tracking; Uncertainty.

1. Introduction

The motion control of uncertain nonholonomic wheeled mobile robots (WMRs) is an attractive research area because of the challenging theoretical nature of the problem according to the well-known Brockett's theorem.[1] Such systems are referred to a class of WMRs without any precise knowledge of their models which are also subjected to nonholonomic constraints that arise from pure rolling without slipping constraint of their wheels. In fact, since nonholonomic WMRs are underactuated systems, i.e. systems with fewer actuators than the degrees of freedom, designing tracking controllers for such WMRs is more difficult than designing controllers for fully actuated ones. After seminal works in refs. [2–6], a variety of control solutions have been proposed in literature for the tracking control of uncertain nonholonomic WMRs.[7–20]

In spite of extensive researches, most of previously proposed controllers[2–20] require velocity sensors to be implemented on a real WMR. From a practical viewpoint, such sensors may increase the implementation cost and weight of the system. Moreover, most of the commercially available WMRs are not equipped with velocity sensors. One traditional solution to leave out velocity sensors is the designing of output feedback controllers (OFBCs). However, since the separation principle does not hold for nonlinear systems, the designing of OFBCs is still a challenging task and is the subject of current researches. In addition, the nonholonomic constraints of WMRs make the OFB problem more challenging. The problem is even more demanding in the presence of parametric and nonparametric uncertainties in the system models. Do and Pan[21,22] proposed OFBCs for a unicycle-type mobile robot at the torque level using a coordinate transformation to cancel the velocity cross terms in WMR dynamics. However, the model uncertainties are ignored in the design of the controller in mentioned

* Corresponding author. E-mail: khoshnam.shojaee@gmail.com

https://doi.org/10.1017/S0263574714000046 Published online by Cambridge University Press

works. Park *et al.*[23] proposed an adaptive OFBC for a nonholonomic WMR, including the actuator dynamics using the dynamic surface control (DSC) approach. However, determining the regression matrix and satisfying the "linearity in the parameters" assumption in their proposed method is a time-consuming and tedious task. In addition, they ignore the nonparametric uncertainties in the design of the controller. In the previous work of the author,[24] a passivity-based OFBC is proposed for the tracking control of a nonholonomic WMR, including actuator dynamics using the DSC approach. In spite of the effectiveness of the proposed algorithm, its tracking performance degrades for large initial tracking errors due to actuator saturation. Guechi *et al.*[25] proposed OFBC based on a nonlinear predictor for unicycle-type mobile robot. However, their work is only focused on designing the OFBC in the presence of delayed measurements and ignores the WMR dynamic model.

To the best of the author's knowledge, most of the presented works, including OFBCs,[21–25] assume that WMR actuators are able to accept every level of voltage signals and generate the necessary level of torque signals. From a practical viewpoint, the generated control signals may make the actuators go beyond their natural capabilities and their saturation may not be avoidable. This, in turn, may result in poor tracking performance of the proposed controller. Furthermore, long-term saturation may lead to serious physical damages, i.e. thermal or mechanical failures of WMR actuators. One solution to alleviate this problem is the bounding of the closed-loop error variables by applying saturation functions and normalization techniques to the designing of tracking controller. By using these techniques, the stabilization and tracking of nonholonomic WMRs with input saturation are addressed in Huang *et al.*[26] and Su and Zheng.[27] However, the availability of velocity measurements is essential for their proposed controllers.

According to the above-presented literature review, the problem of designing a saturated OFBC (SOFBC) for a nonholonomic WMR has not yet been solved and is the subject of this paper. This means that the developed controller in this paper is the first SOFBC design to solve the trajectory-tracking problem of nonholonomic WMRs in the presence of actuator saturation and in the absence of velocity measurements. For this purpose, a suitable set of output equations is defined which transforms the kinematic and dynamic models of nonholonomic WMRs to a new second-order input–output model. This model helps the designer to directly take the advantage of robotic manipulators control schemes.[28] Many previous works have utilized kinematic and dynamic models to separately design kinematic and dynamic controllers based on backstepping or DSC techniques.[6–9,12–16,21–23] Unfortunately, such techniques complicate the design procedure of an SOFBC based on the previous models of WMR. Compared with previously proposed OFBCs[21–25] for nonholonomic WMRs, the proposed observer-based controller of this paper utilizes saturation functions to effectively reduce the risk of actuator saturation. It makes the mobile robot track a desired trajectory with less control energy and more acceptable tracking performance. This feature is specifically helpful for the amount of battery usage in autonomous mobile robotic systems. The proposed controller is applied to a nonholonomic WMR and simulation results are provided to show the efficacy of the controller. A comparative simulation study is also presented to compare the proposed SOFBC with the previous works. This study shows that the proposed SOFBC of this work cope well with actuator constraints when the initial tracking errors are large and WMR actuators are subjected to saturation. As a result of the above-presented discussions, the contributions of this work are clearly expressed.

The remainder of this paper is organized as follows. In Section 2 the kinematic and dynamic models of the nonholonomic robotic systems are briefly reviewed. The control problem definition and some mathematical preliminaries are presented in this section. In Section 3 a saturated OFB tracking controller is designed based on the passivity property of the nonholonomic robotic system. The Lyapunov-based stability analysis is applied to prove that all signals in the resulting closed-loop system are bounded, and tracking errors and state estimation errors are semi-globally uniformly ultimately bounded (SGUUB). In Section 4 a simulation study is presented to evaluate the effectiveness of the proposed controller for a nonholonomic WMR. Conclusions are given in Section 5.

2. Preliminaries and Problem Statement

2.1. WMR kinematics and dynamics

Consider a class of electrically driven WMR systems subjected to m nonholonomic constraints which is described by the following dynamics[21–24]:

https://doi.org/10.1017/S0263574714000046 Published online by Cambridge University Press

$$\dot{q} = S(q)\, v(t) = s_1(q)\, v_1 + \cdots + s_{n-m}(q)\, v_{n-m}, \tag{1}$$

$$M_1 \dot{v}(t) + C_1(q, \dot{q})\, v(t) + D_m v + G_1(q) + \tau_{d1}(t, q, \dot{q}) = B_1(q)\tau_a, \tag{2}$$

where $q = [q_1,\ q_2, \ldots, q_n]^T$ denotes a vector of n generalized coordinates, $S(q) \in \Re^{n\times(n-m)}$ is the kinematic matrix, $v(t) = [v_1(t),\ v_2(t), \ldots, v_{n-m}(t)]^T$ is a vector of pseudo-velocities of the system, $M_1(q) \in \Re^{(n-m)\times(n-m)}$ is a symmetric positive definite inertia matrix, $C_1(q, \dot{q}) \in \Re^{(n-m)\times(n-m)}$ is the centripetal and Coriolis matrix, $D_m \in \Re^{(n-m)\times(n-m)}$ denotes damping matrix, $G_1(q) \in \Re^{(n-m)}$ is the vector of gravity effects, $\tau_{d1}(t, q, \dot{q}) \in \Re^{(n-m)}$ denotes bounded unstructured uncertainties such as friction and unmodeled dynamics, $B_1(q) \in \Re^{(n-m)\times(n-m)}$ is the input transformation matrix, and $\tau_a \in \Re^{(n-m)}$ is the vector of actuator inputs. To consider the actuator voltage input as the control input, it is assumed that the robot is actuated by $n - m$ brushed DC motors with mechanical gears. By recalling the actuator dynamic equation from Shojaei and Shahri[24] and ignoring the inductance of armature circuit[1] similar to ref. [20], the following transformation between the torque and voltage inputs is obtained:

$$\tau_a = K_{a1}\, u_a - K_{a2} X_1 v\,, \tag{3}$$

where $K_{a1} = \text{diag}[k_{a11}, k_{a12}, \ldots, k_{a1(n-m)}]$, $K_{a2} = \text{diag}[k_{a21}, k_{a22}, \ldots, k_{a2(n-m)}]$, and $k_{a1i} = (n_i k_{\tau i}/r_{ai})$ and $k_{a2i} = n_i\, k_{bi} k_{a1i}$, $i = 1, 2, \ldots, n-m$, n_i denotes the gear ratio, $k_{\tau i}$ is the torque constant of the motor, r_{ai} denotes the armature resistance, k_{bi} is the back electromotive force (EMF) constant, $X_1 \in \Re^{(n-m)\times(n-m)}$ is a transformation matrix that transforms wheel velocities to pseudo-velocities vector, and τ_a and $u_a \in \Re^{(n-m)}$ denote the torque and voltage input vectors respectively. After substituting Eq. (3) in Eq. (2), one obtains

$$M_1(q)\dot{v}(t) + (C_1(q, \dot{q}) + K_{a2} B_1(q) X_1(q))\, v(t) + D_m v(t) + G_1(q) + \tau_{d1}(t, q, \dot{q}) = K_{a1} B_1(q)\, u_a, \tag{4}$$

where $\tau_{d1}(t, q, \dot{q}) = D_1 v(t) + D_2 \text{sgn}(v(t)) + d(t)$, and the reader is referred to remark 1 in ref. [24] for the definition of $\tau_{d1} \in \Re^{n-m}$, $D_1,\ D_2 \in \Re^{(n-m)\times(n-m)}$, and $d(t) \in \Re^{n-m}$.

Notations. Throughout this paper, $\lambda_{\max}(\bullet)$ ($\lambda_{\min}(\bullet)$) denotes the largest (smallest) eignevalue of a matrix. $\|x\| := \sqrt{x^T x}$ is used as the Euclidean norm of vector $x \in \Re^n$, while the norm of matrix A is defined as the induced norm $\|A\| := \sqrt{\lambda_{\max}(A^T A)}$. The matrix I_n denotes the n-dimensional identity matrix. To facilitate the subsequent control design and stability analysis, the following notations are also used: $s'(\eta) = \text{diag}[s'_1(\eta_1), \ldots, s'_n(\eta_n)]$ and $s(\eta) := [s_1(\eta_1),\ s_2(\eta_2), \ldots, s_n(\eta_n)]^T$, where $\eta = [\eta_1,\ \eta_2, \ldots, \eta_n]^T \in \Re^n$, diag $[\bullet]$ denotes a diagonal matrix, $s_i(\bullet)$, $i = 1, \ldots, n$ and $s'_i(\bullet)$, $i = 1, \ldots, n$ are saturation functions and their derivatives, respectively, which are defined later.

Property 1. $M_1(q)$ is a symmetric and positive-definite matrix which is upper and lower bounded such that $\lambda_{m_1}\|x\|^2 \le x^T M_1(q) x \le \lambda_{M_1}\|x\|^2\ \forall q,\ x \in \Re^n$, and $0 < \lambda_{m_1} \le \lambda_{M_1} < \infty$, where $\lambda_{m_1} := \min_{\forall q\in\Re^n} \lambda_{\min}(M_1(q))$ and $\lambda_{M_1} := \max_{\forall q\in\Re^n} \lambda_{\max}(M_1(q))$.

Property 2. The following upper bounding functions are valid for the presented kinematic and dynamic models of nonholonomic systems:

$$\begin{aligned} &\|S(q)\| \le \lambda_S,\quad \|C_1(q, \dot{q})\| \le \lambda_{C_1}\|v\|\,,\ \|B_1(q)\| \le \lambda_{B_1},\ \|X_1(q)\| \le \lambda_{X_1}, \\ &\|D_m\| \le \lambda_{D_m},\ \|G_1(q)\| \le \lambda_{G_1},\ \|\tau_{d1}\| \le \lambda_{\tau_1} + \lambda_{\tau_2}\|v\|\,,\ \forall q,\ \dot{q} \in \Re^n,\ \forall v \in \Re^{n-m}, \end{aligned} \tag{5}$$

where $\lambda_S,\ \lambda_{C_1}, \lambda_{B_1}, \lambda_{X_1}, \lambda_{D_m}, \lambda_{\tau_1}, \lambda_{\tau_2}$, and λ_{G_1} are positive scalar constants.

[1] The reader is referred to remark 1 in ref. [20] for the validity of this assumption.

https://doi.org/10.1017/S0263574714000046 Published online by Cambridge University Press

2.2. Reduced model of a nonholonomic WMR

For the controller design purposes in the next section, it is assumed that there exist the following smooth output equations:

$$y = h(q) = [h_1(q),\ h_2(q), \ldots,\ h_{n-m}(q)]^T, \tag{6}$$

where $y \in \Re^{n-m}$ is a new position variable. By differentiating the output Eq. (6) and substituting Eq. (1), one gets

$$\dot{y} = J(q)\, v, \tag{7}$$

where $J(q) := J_h(q)S(q) \in \Re^{(n-m)\times(n-m)}$, which is assumed to be invertible, and $J_h(q) := \partial h(q)/\partial q$.[24] By following model derivation in Shojaei and Shahri,[24] the following reduced formulation of nonholonomic WMRs is obtained:

$$M_2(q)\ddot{y} + C_2(q, \dot{y})\dot{y} + X_2(q)\dot{y} + G_2(q) + \tau_{d2}(t, q, \dot{y}) = B_2(q)\, u_a, \tag{8}$$

where

$$\begin{aligned}
M_2(q) &= K_{a1}^{-1} J^{-T}(q) M_1(q)\, J^{-1}(q),\\
C_2(q, \dot{y}) &= K_{a1}^{-1} J^{-T}(q)(C_1(q, S(q)J^{-1}(q)\dot{y})\ -\ M_1(q)\, J^{-1}(q)\dot{J}(q))J^{-1}(q),\\
X_2(q) &= K_{a1}^{-1} J^{-T}(q)(K_{a2}\, B_1(q)X_1(q)\ +\ D_m\ +\ D_1)J^{-1}(q),\\
G_2(q) &= K_{a1}^{-1} J^{-T}(q)G_1(q),\ \ B_2(q) = J^{-T}(q)B_1(q),\\
\tau_{d2}(t, q, \dot{y}) &= K_{a1}^{-1} J^{-T}(q)(D_2 \mathrm{sgn}(J^{-1}(q)\dot{y}) + d(t)).
\end{aligned}$$

This representation of a nonholonomic WMR is essential for controller development in the next section. The following properties are valid for the model in Eq. (8).

Property 3. $M_2(q)$ is a symmetric and positive-definite matrix which is upper and lower bounded such that $\lambda_{m_2}\|x\|^2 \le x^T M_2(q)x \le \lambda_{M_2}\|x\|^2\ \forall q \in \Re^n,\ \forall x \in \Re^{n-m}$, and $0 < \lambda_{m_2} \le \lambda_{M_2} < \infty$ where $\lambda_{m_2} := \min_{\forall q\in\Re^n} \lambda_{\min}(M_2(q))$ and $\lambda_{M_2} := \max_{\forall q\in\Re^n} \lambda_{\max}(M_2(q))$.

Property 4. Matrix $\dot{M}_2 - 2\,C_2$ is skew symmetric, i.e.

$$x^T(\dot{M}_2(q) - 2\,C_2(q, \dot{y}))x = 0,\ \ \forall\, q \in \Re^n,\ \ \forall\, \dot{y}, x \in \Re^{n-m}. \tag{9}$$

Property 5. The centripetal-Coriolis matrix satisfies the following relationship:

$$C_2(q, x_1)x_2 = C_2(q, x_2)x_1,\ \ \forall\, q \in \Re^n,\ \ \forall\, x_1, x_2 \in \Re^{n-m}. \tag{10}$$

Property 6. Based on property 2, there exists positive scalar constants $\lambda_J, \lambda_{C_2}, \lambda_{G_2}, \lambda_{\tau_{d2}}$ and λ_{B_2} such that

$$\begin{aligned}
&\|J(q)\| \le \lambda_J,\ \ \|C_2(q, \dot{y})\| \le \lambda_{C_2}\,\|\dot{y}\|,\ \ \|G_2(q)\|\ \le \lambda_{G_2},\\
&\|\tau_{d2}(t, q, \dot{y})\| \le \lambda_{\tau_{d2}},\ \|B_2(q)\| \le \lambda_{B_2},\ \ \forall q \in \Re^n,\ \ \forall\, \dot{y} \in \Re^{n-m}.
\end{aligned} \tag{11}$$

Property 7. The matrix $X_2(q)$ in Eq. (8) satisfies $\lambda_{x_2}\|x\|^2 \le x^T X_2(q)x \le \lambda_{X_2}\|x\|^2\ \forall\, x \in \Re^{n-m}$, and $0 < \lambda_{x_2} \le \lambda_{X_2} < \infty$, where $\lambda_{x_2} := \min_{\forall q\in\Re^n} \lambda_{\min}(X_2(q))$ and $\lambda_{X_2} := \max_{\forall q\in\Re^n} \lambda_{\max}(X_2(q))$.

2.3. Mathematical preliminaries

The following control objective is addressed in this paper.

Definition 1. Given a smooth bounded reference trajectory $y_d(t) = h(q_d(t)) : [0, \infty) \to \Re^n$, which is generated by an associated timing law, the *control objective* discussed in this paper is to

https://doi.org/10.1017/S0263574714000046 Published online by Cambridge University Press

design an SOFBC law for the uncertain nonholonomic WMR system given by Eqs. (1), (2), and (3) such that (*i*) it makes the tracking errors, $e(t) := y(t) - y_d(t)$, uniformly ultimately bounded in the presence of structured and unstructured uncertainties; (*ii*) it does not require measurements of the velocity signals; and (*iii*) it alleviates the actuator saturation problem in order to avoid poor tracking performance.

Definition 2. Given a positive constant M_i, a function $s_i : \Re \to \Re : \xi \to s_i(\xi)$ is said to be a saturation one with bound M_i if it is locally Lipschitz, nondecreasing, and satisfies the following: (*i*) $\xi s_i(\xi) > 0, \ \forall \xi \neq 0$; and (*ii*) $|s_i(\xi)| \leq M_i, \ \forall \xi \in \Re$. A strictly increasing continuously differentiable function satisfying the above definition has the following properties.

Lemma 1. Let $s_i : \Re \to \Re : \xi \to s_i(\xi)$ be a strictly increasing, continuously differentiable saturation function with bound M_i, k_1 and k_2 be positive constants, and $s_i' : \xi \to ds_i/d\xi$. Then the following properties can be proved:

(i) $y[s_i(x + y) - s_i(x)] > 0, \ \forall y \neq 0, \ \forall x \in \Re$.
(ii) $\lim_{|\xi| \to \infty} s_i'(\xi) = 0$.
(iii) $s_i'(\xi)$ is positive and bounded, i.e. there exists a constant $s_{iM}' \in (0, \infty)$ such that $0 < s_i'(\xi) \leq s_{iM}', \ \forall \xi \in \Re$.
(iv) $s_i^2(k_1\xi)/(2k_1 s_{iM}') \leq \int_0^{\xi} s_i(k_1 r)dr \leq k_1 s_{iM}' \xi^2/2, \ \forall \xi \in \Re$.
(v) $\int_0^{\xi} s_i(kr)dr > 0, \ \forall \xi \neq 0$.
(vi) $\int_0^{\xi} s_i(kr)dr \to \infty$ as $|\xi| \to \infty$.
(vii) $|s_i(k_1 x + k_2 y) - s_i(k_2 y)| \leq s_{iM}' k_1 |x|, \ \forall x, \ y \in \Re$ and $|s_i(x) - s_i(x - y)| \leq s_{iM}' |y|, \ \forall x, \ y \in \Re$.
(viii) $|s_i(k_1 x)| \leq s_{iM}' k_1 |x|, \ \forall x \in \Re$.
(ix) From item (viii), it follows that $|s_i(x)|^2 \leq s_{iM}' |x||s_i(x)| = s_{iM}' x \, s_i(x), \ \forall x \in \Re$.
(x) From item (iv), it follows that $s_i^2(\xi) \leq s_{iM}'^2 \xi^2, \ \forall \xi \in \Re$.
(xi) From item (iii), it is concluded that $\|s'(\eta)\| \leq s_{MM}', \ \forall \eta \in \Re^n$, where $s_{MM}' := \lambda_{\max}(s_M')$ and $s_M' = \text{diag}[s_{1M}', \ldots, s_{nM}']$.

Proof. See Aguinaga-Ruiz *et al.*[30]

Following assumptions are essential to meet the control objectives in this paper:

Assumption 1. Measurements of output vector $y \in \Re^{n-m}$ are available in real-time.

Assumption 2. The desired trajectory $y_d(t)$ is chosen such that $y_d(t)$, $\dot{y}_d(t)$, and $\ddot{y}_d(t)$ are all bounded signals in the sense that $\sup_{t \geq 0} \|y_d\| < B_{dp}$, $\sup_{t \geq 0} \|\dot{y}_d\| < B_{dv}$, and $\sup_{t \geq 0} \|\ddot{y}_d\| < B_{da}$, where B_{dp}, B_{dv}, and B_{da} are bounded constants.

The reader is also referred to assumption 3 in Shojaei and Shahri.[24]

3. SOFBC Design and Analysis

3.1. Saturated output feedback tracking control law

In this section a trajectory tracking controller is designed based on the control objective defined in Definition 1. For this purpose, define the observation error as $z := y - \hat{y}$ and consider the following definitions:

$$\dot{y}_r := \dot{y}_d - \Lambda \, s(\hat{y} - y_d) = \dot{y}_d - \Lambda \, s(e - z), \tag{12}$$

$$r_1 := \dot{y} - \dot{y}_r = \dot{e} + \Lambda \, s(e - z), \tag{13}$$

$$\dot{y}_o := \dot{\hat{y}} - \Lambda \, s(z), \tag{14}$$

$$r_2 := \dot{y} - \dot{y}_o = \dot{z} + \Lambda \, s(z), \tag{15}$$

https://doi.org/10.1017/S0263574714000046 Published online by Cambridge University Press

where $\Lambda = \lambda I_{n-m} \in \Re^{(n-m)\times(n-m)}$ with $\lambda > 0$. By substituting Eq. (13) in Eq. (8) and applying Property 5, one obtains

$$M_2(q)\dot{r}_1 = -C_2(q, \dot{y})r_1 - X_2 r_1 + B_2 u_a - C_2(q, \dot{y}_r)r_1 + \xi, \tag{16}$$

where $\xi = -M_2(q)\ddot{y}_r - C_2(q, \dot{y}_r)\dot{y}_r - X_2\dot{y}_r - G_2(q) - \tau_{d2}(t, q, \dot{y})$ denotes the uncertain nonlinearities, which may be bounded as $\|\xi\| \le \rho(\dot{y}_r, \ddot{y}_r) = G(\dot{y}_r, \ddot{y}_r)\theta$ by using Properties 3 and 6, where $G(\dot{y}_r, \ddot{y}_r) = [\,1 \;\|\dot{y}_r\| \;\|\dot{y}_r\|^2 \;\|\ddot{y}_r\|\,]$. Then the following tracking controller is proposed:

$$\begin{aligned} u_a = B_2^{-1}(q)(&-K_1 s(\dot{y}_o - \dot{y}_r) - K_2 s(e - z) \\ &-K_2 s(z) - \hat{\rho}(\dot{y}_r, \ddot{y}_r) s(\nu\hat{\rho}(r_1 + r_2)/\varepsilon_t)), \end{aligned} \tag{17}$$

where $K_1, K_2 \in \Re^{(n-m)\times(n-m)}$ are positive-definite diagonal gain matrices, $\hat{\rho}(\dot{y}_r, \ddot{y}_r) = G(\dot{y}_r, \ddot{y}_r)\hat{\theta}$ is the estimate of the upper bounding function $\rho(\dot{y}_r, \ddot{y}_r)$, and $\hat{\theta} \in \Re^4$ is updated by the following adaptation rule with σ-modification[32]:

$$\dot{\hat{\theta}} = \Gamma\, G^T(\dot{y}_r, \ddot{y}_r)\, \|r_1 + r_2\| - \Gamma\, \sigma\, (\hat{\theta} - \theta_0), \tag{18}$$

where $\Gamma = \gamma I_4$ denotes the adaptation gain, $\sigma \in \Re^4$ is a positive-definite diagonal matrix, and $\theta_0 \in \Re^4$ is *a priori* estimate of the parameters. Motivated by Arteaga and Kelly,[33] the following nonlinear saturated observer is introduced to estimate the velocity vector:

$$\dot{\hat{y}} = \dot{\hat{y}}_o + \Lambda\, s(z) + k_d\, s(z), \tag{19}$$

$$\ddot{\hat{y}}_o = \ddot{y}_r + k_d \Lambda s'(z(t))s(z(t)), \tag{20}$$

where $k_d \in \Re$ is the observer gain and is a positive real constant. Equation (7) can be applied to compute the velocity estimates as $\hat{v} = J^{-1}(q)\dot{\hat{y}}$. Considering the definition of $\dot{y}_r$ in Eq. (12), $\ddot{y}_r$ is available for the observer definition. The initial conditions for the observer are chosen as $\dot{\hat{y}}_o(0) = -(\Lambda s(z(0)) + k_d s(z(0)))$, $\hat{y}(0) = y(0)$, $z(0) = 0$, and $\dot{\hat{y}}(0) = 0$.

3.2. Closed-loop error dynamic analysis

Considering that $r_1 - r_2 = \dot{y}_o - \dot{y}_r$ from Eqs. (13) and (15), and substituting Eq. (17) into Eq. (16), the closed-loop system dynamics may be achieved as

$$\begin{aligned} M_2(q)\dot{r}_1 = &-C_2(q, \dot{y})r_1 - X_2 r_1 - K_1 s(r_1 - r_2) - K_2 s(e - z) \\ &-K_2 s(z) - \hat{\rho} s(\nu\hat{\rho}(r_1 + r_2)/\varepsilon_t) - C_2(q, \dot{y}_r)r_1 + \xi, \end{aligned} \tag{21}$$

where one may write the following upper bound for $C_2(q, \dot{y}_r)r_1$:

$$\|C_2(q, \dot{y}_r)r_1\| \le \zeta_1 \|x\| + \zeta_2 \|x\|^2, \tag{22}$$

where $\zeta_1,\ \zeta_2 \in \Re$ are some positive bounding constants and $x \in \Re^{4(n-m)}$ is defined as

$$x = \left[s^T(e - z), s^T(z),\ r_1^T,\ r_2^T\right]^T. \tag{23}$$

Since from Eq. (19) one can write $\ddot{\hat{y}} = \ddot{\hat{y}}_o + \Lambda\, s'(z)\dot{z} + k_d\, s'(z)\dot{z}$, it is straightforward to show that Eqs. (19) and (20) are equivalent to $\dot{r}_1 = \dot{r}_2 + k_d\, s'(z)r_2$, which together with Eq. (21) and Property 5 yield the following observer error equation:

$$\begin{aligned} M_2(q)\dot{r}_2 = &-C_2(q, \dot{y})r_2 - k_d M_2(q)\, s'(z)r_2 - K_1 s(r_1 - r_2) - K_2 s(e - z) \\ &- K_2 s(z) - \hat{\rho} s(\nu\hat{\rho}(r_1 + r_2)/\varepsilon_t) + \chi_2 + \xi, \end{aligned} \tag{24}$$

https://doi.org/10.1017/S0263574714000046 Published online by Cambridge University Press

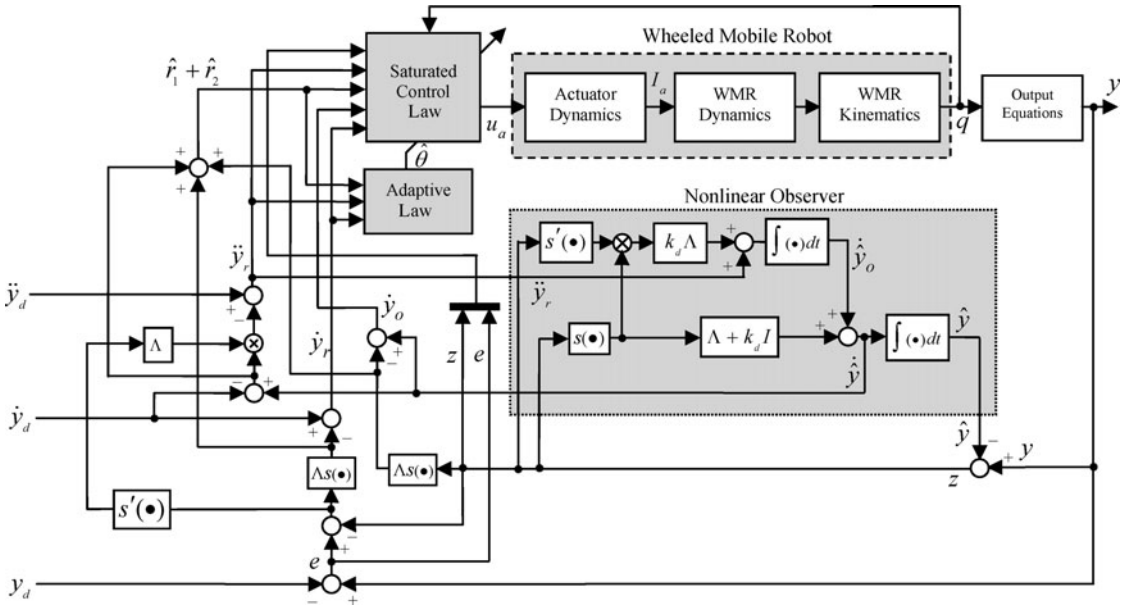

Fig. 1. A detailed block diagram of the proposed saturated output feedback control system.

where

$$\chi_2 = C_2(q, \dot{y}_r + r_1)r_2 - C_2(q, r_1)(2\dot{y}_r + r_1) - X_2 r_1. \tag{25}$$

From Eqs. (12)–(15), Lemma 1, and Properties 6 and 7, the following upper bound for $\chi_2(e, z, r_1, r_2)$ is obtained:

$$\|\chi_2\| \leq \zeta_3 \|x\| + \zeta_4 \|x\|^2, \tag{26}$$

where $\zeta_3,\ \zeta_4 \in \Re$ are some positive bounding constants. Figure 1 shows a block diagram of the proposed SOFBC system.

3.3. Stability analysis

The stability of the proposed saturate OFB tracking controller is summarized by the following theorem.

Theorem 1. Consider the reduced model of the nonholonomic wheeled mobile robot, which is given by Eq. (8). Given a bounded continuous desired trajectory under Assumptions 1 and 2, if gains of SOFBC in Eqs. (17)–(20) are chosen to satisfy the following conditions,

$$\lambda_{\min}(K_2\Lambda) > 0.5k_{2\max}\lambda + k_{2\max}, \tag{27}$$

$$\lambda_{x_2} > s'_{MM}k_{1\max} + 0.5k_{2\max} + 0.5(\zeta_1 + \zeta_2), \tag{28}$$

$$\lambda_{\min}(k_d M_2 s'(z)) > 2s'_{MM}k_{1\max} + k_{2\max} + 0.5(\zeta_3 + \zeta_4), \tag{29}$$

where $k_{i\max} = \lambda_{\max}(K_i),\ i = 1, 2$, then the SOFBC guarantees that all signals in the closed-loop system are bounded and the tracking and observation errors are SGUUB and exponentially converge to small ball containing the origin whose radius can be made arbitrarily small. Moreover, the following region of attraction can be made arbitrarily large to include any initial conditions by selecting the control gains large enough,

$$R_A = \left\{ \vartheta \in \Re^{4(n-m)+4} \;\middle|\; \|\vartheta\| < \sqrt{\frac{2\alpha_m - (\zeta_1 + \zeta_3)}{(\zeta_2 + \zeta_4)\min\{\lambda_\upsilon/\lambda_x, 0.5\lambda_{\max}(\Gamma^{-1})/\lambda_x\}}} \right\}, \tag{30}$$

https://doi.org/10.1017/S0263574714000046 Published online by Cambridge University Press

where $\vartheta = [\upsilon^T,\ \tilde{\theta}^T]^T$, $\upsilon = [(e-z)^T, z^T,\ r_1^T,\ r_2^T]^T$, $\tilde{\theta} = \theta - \hat{\theta}$ denotes the vector of parameters estimation error, α_m is a positive gain-dependent parameter, $\zeta_i,\ i = 1, \ldots, 4$ are defined by Eqs. (22) and (26), $x \in \Re^{4(n-m)}$ was defined in Eq. (23), and $\lambda_x, \lambda_\upsilon$ will be defined later.

Proof. Consider the following Lyapunov function candidate:

$$V(t) = \sum_{i=1}^{n-m} k_{2i} \int_0^{e_i - z_i} s_i(r)\, dr + \frac{1}{2} r_1^T M_2(q) r_1 + \sum_{i=1}^{n-m} k_{2i} \int_0^{z_i} s_i(r)\, dr + \frac{1}{2} r_2^T M_2(q) r_2 + \frac{1}{2} \tilde{\theta}^T \Gamma^{-1} \tilde{\theta}. \tag{31}$$

By utilizing item (*iv*) of Lemma 1, one may verify that Eq. (31) can be bounded as follows:

$$\begin{aligned} &\sum_{i=1}^{n-m} k_{2i} s_i^2(e_i - z_i)/(2s'_{iM}) + \frac{1}{2}\lambda_{m_2} \|r_1\|^2 + \sum_{i=1}^{n-m} k_{2i} s_i^2(z_i)/(2s'_{iM}) + \frac{1}{2}\lambda_{m_2} \|r_2\|^2 + \frac{1}{2}\lambda_{\min}(\Gamma^{-1})\|\tilde{\theta}\|^2 \\ &\le V(t) \le \frac{1}{2} \max\{k_{21}s'_{1M}, \ldots, k_{2n}s'_{nM}\} \|e - z\|^2 + \frac{1}{2}\lambda_{M_2} \|r_1\|^2 + \frac{1}{2} \max\{k_{21}s'_{1M}, \ldots, k_{2n}s'_{nM}\} \|z\|^2 \\ &+ \frac{1}{2}\lambda_{M_2} \|r_2\|^2 + \frac{1}{2}\lambda_{\max}(\Gamma^{-1}) \left\|\tilde{\theta}\right\|^2, \end{aligned} \tag{32}$$

which can be expressed as follows:

$$\lambda_x \|x\|^2 + 0.5\lambda_{\min}(\Gamma^{-1})\|\tilde{\theta}\|^2 \le V(t) \le \lambda_\upsilon \|\upsilon\|^2 + 0.5\lambda_{\max}(\Gamma^{-1}) \left\|\tilde{\theta}\right\|^2, \tag{33}$$

where $\lambda_x = \min\{\lambda_{ks,\min},\ \lambda_{m_2}/2\}$, $\lambda_\upsilon = \max\{\lambda_{ks,\max}, \lambda_{M_2}/2\}$,

$$\lambda_{ks,\min} = \frac{1}{2} \min\{k_{21}/s'_{1M}, \ldots, k_{2(n-m)}/s'_{(n-m)M}\}, \quad \lambda_{ks,\max} = \frac{1}{2} \max\{k_{21}s'_{1M}, \ldots, k_{2(n-m)}s'_{(n-m)M}\},$$

and λ_{m_2} and λ_{M_2} are defined in Property 3. From the above inequality and items (*v*) and (*vi*) of Lemma 1, it is clear that $V(t)$ is positive definite, radially unbounded, and decrescent. By differentiating Eq. (31) along Eqs. (13), (15), (21), and (24), using Property 4 and the fact that $\dot{\hat{\theta}} = -\dot{\tilde{\theta}}$, we have

$$\begin{aligned} \dot{V}(t) &= s^T(e-z)K_2(\dot{e} - \dot{z}) + r_1^T M_2 \dot{r}_1 + 0.5 r_1^T \dot{M}_2 r_1 + s^T(z)K_2\dot{z} \\ &\quad + r_2^T M_2 \dot{r}_2 + 0.5 r_2^T \dot{M}_2 r_2 - \tilde{\theta}^T \Gamma^{-1} \dot{\hat{\theta}} \\ &= -s^T(e-z)K_2\Lambda\, s(e-z) - s^T(z)K_2\Lambda\, s(z) - r_1^T X_2 r_1 \\ &\quad - k_d r_2^T M_2(q)\, s'(z) r_2 - r_1^T K_1 s(r_1 - r_2) - r_2^T K_1 s(r_1 - r_2) \\ &\quad + s^T(e-z)K_2\Lambda\, s(z) - r_1^T K_2\, s(z) - 2 r_2^T K_2\, s(e-z) \\ &\quad - \hat{\rho}(r_1 + r_2)^T s(\nu\hat{\rho}(r_1 + r_2)/\varepsilon_t) - r_1^T C_2(q, \dot{y}_r) r_1 + r_2^T \chi_2 \\ &\quad + r_1^T \xi + r_2^T \xi - \tilde{\theta}^T \Gamma^{-1} \dot{\hat{\theta}}. \end{aligned} \tag{34}$$

After rearrangement, Eq. (34) is written as follows:

$$\begin{aligned} \dot{V}(t) \le &- s^T(e-z)K_2\Lambda\, s(e-z) - s^T(z)K_2\Lambda\, s(z) - r_1^T X_2 r_1 \\ &- k_d r_2^T M_2(q)\, s'(z) r_2 + r_1^T K_1(s(r_1) - s(r_1 - r_2)) - r_1^T K_1 s(r_1) \\ &+ r_2^T K_1(s(r_1) - s(r_1 - r_2)) - r_2^T K_1 s(r_1) + \|K_2\Lambda\|\, \|s(e-z)\|\, \|s(z)\| \\ &+ \|K_2\|\, \|r_1\|\, \|s(z)\| + 2\|K_2\|\, \|r_2\|\, \|s(e-z)\| + \|r_1\|\, \|C_2(q, \dot{y}_r) r_1\| + \|r_2\|\, \|\chi_2\| \\ &- \hat{\rho}(r_1 + r_2)^T s(\nu\hat{\rho}(r_1 + r_2)/\varepsilon_t) + (r_1 + r_2)^T \xi - \tilde{\theta}^T \Gamma^{-1} \dot{\hat{\theta}}. \end{aligned} \tag{35}$$

https://doi.org/10.1017/S0263574714000046 Published online by Cambridge University Press

By substituting the adaptive law in Eq. (18) into inequality (35), one obtains

$$\begin{aligned}\dot{V}(t) \leq & -s^T(e-z)K_2\Lambda\, s(e-z) - s^T(z)K_2\Lambda\, s(z) - r_1^T X_2 r_1 \\ & - k_d r_2^T M_2(q)\, s'(z) r_2 + \|K_1\|\,\|r_1\|\,\|s(r_1) - s(r_1 - r_2)\| - r_1^T K_1 s(r_1) \\ & + \|K_1\|\,\|r_2\|\,\|s(r_1) - s(r_1 - r_2)\| + \|K_1\|\,\|r_2\|\,\|s(r_1)\| + \|K_2\Lambda\|\,\|s(e-z)\|\,\|s(z)\| \\ & + \|K_2\|\,\|r_1\|\,\|s(z)\| + 2\,\|K_2\|\,\|r_2\|\,\|s(e-z)\| + \|r_1\|\,\|C_2(q,\dot{y}_r)r_1\| + \|r_2\|\,\|\chi_2\| \\ & - \hat{\rho}(r_1+r_2)^T s(\nu\hat{\rho}(r_1+r_2)/\varepsilon_t) + \|r_1+r_2\|\,\|\xi\| - \tilde{\theta}^T\, G^T(\dot{y}_r,\ \ddot{y}_r)\,\|r_1+r_2\| \\ & + \tilde{\theta}^T\,\sigma\,(\hat{\theta} - \theta_0). \end{aligned} \tag{36}$$

By considering items (*vii*), (*viii*), and (*ix*) of Lemma 1, and recalling the upper bounds on $\|\xi\|$, $\|C_2(q,\dot{y}_r)r_1\|$, and $\|\chi_2\|$, one gets

$$\begin{aligned}\dot{V}(t) \leq & -\lambda_{\min}(K_2\Lambda)\,\|s(e-z)\|^2 - \lambda_{\min}(K_2\Lambda)\,\|s(z)\|^2 - \lambda_{x_2}\|r_1\|^2 \\ & - \lambda_{\min}(k_d M_2\, s'(z))\,\|r_2\|^2 - \lambda_{\min}(K_1)/s'_{MM}\,\|s(r_1)\|^2 \\ & + s'_{MM}\,\|K_1\|\,\|r_1\|\,\|r_2\| + s'_{MM}\,\|K_1\|\,\|r_2\|^2 + s'_{MM}\,\|K_1\|\,\|r_1\|\,\|r_2\| \\ & + \|K_2\Lambda\|\,\|s(e-z)\|\,\|s(z)\| + \|K_2\|\,\|r_1\|\,\|s(z)\| + 2\,\|K_2\|\,\|r_2\|\,\|s(e-z)\| \\ & + \zeta_1\,\|r_1\|\,\|x\| + \zeta_2\,\|r_1\|\,\|x\|^2 + \zeta_3\,\|r_2\|\,\|x\| + \zeta_4\,\|r_2\|\,\|x\|^2 \\ & + \|r_1+r_2\|\,G(\dot{y}_r,\ \ddot{y}_r)\theta - \tilde{\theta}^T\, G^T(\dot{y}_r,\ \ddot{y}_r)\,\|r_1+r_2\| \\ & - \hat{\rho}(r_1+r_2)^T s(\nu\hat{\rho}(r_1+r_2)/\varepsilon_t) + \tilde{\theta}^T\,\sigma\,(\hat{\theta} - \theta_0), \end{aligned} \tag{37}$$

where s'_{MM} was defined by item (*xi*) of Lemma 1. By considering Young's inequality,[14] since

$$\begin{aligned} & 2s'_{MM}\,\|K_1\|\,\|r_1\|\,\|r_2\| \leq s'_{MM}k_{1\max}\,\|r_1\|^2 + s'_{MM}k_{1\max}\,\|r_2\|^2, \\ & \|K_2\Lambda\|\,\|s(e-z)\|\,\|s(z)\| \leq 0.5k_{2\max}\lambda\,\|s(e-z)\|^2 + 0.5k_{2\max}\lambda\,\|s(z)\|^2, \\ & \|K_2\|\,\|r_1\|\,\|s(z)\| \leq 0.5k_{2\max}\,\|r_1\|^2 + 0.5k_{2\max}\,\|s(z)\|^2, \\ & 2\,\|K_2\|\,\|r_2\|\,\|s(e-z)\| \leq k_{2\max}\,\|r_2\|^2 + k_{2\max}\,\|s(e-z)\|^2, \end{aligned}$$

one may write inequality (37) as follows:

$$\begin{aligned}\dot{V}(t) \leq & -\lambda_{\min}(K_2\Lambda)\,\|s(e-z)\|^2 - \lambda_{\min}(K_2\Lambda)\,\|s(z)\|^2 - \lambda_{x_2}\|r_1\|^2 \\ & - \lambda_{\min}(k_d M_2\, s'(z))\,\|r_2\|^2 - \lambda_{\min}(K_1)/s'_{MM}\,\|s(r_1)\|^2 \\ & + (0.5k_{2\max}\lambda + k_{2\max})\,\|s(e-z)\|^2 + (0.5k_{2\max}\lambda + 0.5k_{2\max})\,\|s(z)\|^2 \\ & + (s'_{MM}k_{1\max} + 0.5k_{2\max})\,\|r_1\|^2 + (2s'_{MM}k_{1\max} + k_{2\max})\,\|r_2\|^2 \\ & + 0.5(\zeta_1+\zeta_2)\,\|r_1\|^2 + 0.5(\zeta_3+\zeta_4)\,\|r_2\|^2 + 0.5(\zeta_1+\zeta_3)\,\|x\|^2 \\ & + 0.5(\zeta_2+\zeta_4)\,\|x\|^4 + \|r_1+r_2\|\,G(\dot{y}_r,\ \ddot{y}_r)\hat{\theta} \\ & - \hat{\rho}(r_1+r_2)^T s(\nu\hat{\rho}(r_1+r_2)/\varepsilon_t) + \tilde{\theta}^T\,\sigma\,(\hat{\theta} - \theta_0). \end{aligned} \tag{38}$$

By recalling the fact $h\|x\| - x^{\mathrm{T}}h\, s(\nu h\, x/\varepsilon_t) \leq n\varepsilon_t, \forall x \in \Re^n,\ h \in \Re,\ \varepsilon_t > 0$ from refs. [20, 31], inequality (38) may be expressed as follows:

$$\begin{aligned}\dot{V}(t) \leq & -\alpha_1\,\|s(e-z)\|^2 - \alpha_2\,\|s(z)\|^2 - \alpha_3\,\|r_1\|^2 - \alpha_4\,\|r_2\|^2 \\ & - \lambda_{\min}(K_1)/s'_{MM}\,\|s(r_1)\|^2 + 0.5(\zeta_1+\zeta_3)\,\|x\|^2 + 0.5(\zeta_2+\zeta_4)\,\|x\|^4 \\ & + (n-m)\varepsilon_t + \tilde{\theta}^T\,\sigma\,(\hat{\theta} - \theta_0), \end{aligned} \tag{39}$$

https://doi.org/10.1017/S0263574714000046 Published online by Cambridge University Press

where $\alpha_i,\ i = 1, \ldots, 4$ are defined as

$$\begin{aligned}
\alpha_1 &= \lambda_{\min}(K_2\Lambda) - 0.5k_{2\max}\lambda - k_{2\max},\\
\alpha_2 &= \lambda_{\min}(K_2\Lambda) - 0.5k_{2\max}\lambda - 0.5k_{2\max},\\
\alpha_3 &= \lambda_{x_2} - s'_{MM}k_{1\max} - 0.5k_{2\max} - 0.5(\zeta_1 + \zeta_2),\\
\alpha_4 &= \lambda_{\min}(k_d M_2\, s'(z)) - 2s'_{MM}k_{1\max} - k_{2\max} - 0.5(\zeta_3 + \zeta_4).
\end{aligned} \tag{40}$$

The control gains must be chosen such that $\alpha_i > 0,\ i = 1, \ldots, 4$, which, in turn, result in the conditions in Eqs. (27)–(29). By completing the squares on the last term of inequality (39), it is written as follows:

$$\begin{aligned}
\dot{V}(t) \leq &-(\alpha_m - 0.5(\zeta_1 + \zeta_3) - 0.5(\zeta_2 + \zeta_4)\|x\|^2)\|x\|^2\\
&- \mu_\sigma(1 - 0.5/\kappa^2)\|\tilde{\theta}\|^2 + \gamma(t),
\end{aligned} \tag{41}$$

where $x \in \Re^{4(n-m)}$ is defined by Eq. (23) and $\alpha_m = \min\{\alpha_1,\ \alpha_2, \alpha_3, \alpha_4\}, \gamma(t) = 0.5\mu_\sigma\kappa^2||\theta - \theta_0||^2 + (n-m)\varepsilon_t(t)$, $\mu_\sigma = \sqrt{\lambda_{\min}(\sigma^T\sigma)}$, and $\kappa \in \Re$ is a positive constant such that $\kappa > \sqrt{2}/2$. Hence, if α_m is chosen such that

$$\alpha_m > 0.5(\zeta_1 + \zeta_3) + 0.5(\zeta_2 + \zeta_4)\|x\|^2, \tag{42}$$

then inequality (41) can be expressed as

$$\dot{V}(t) \leq -c_m\|x\|^2 - \mu_\sigma(1 - 0.5/\kappa^2)\|\tilde{\theta}\|^2 + \gamma(t), \tag{43}$$

where $c_m \in \Re$ is some positive constant. Inequality (43) can be expressed as follows:

$$\dot{V}(t) \leq -c\|\eta(t)\|^2 + \gamma(t), \tag{44}$$

where $c = \min\{c_m,\ \mu_\sigma(1 - 0.5/\kappa^2)\}$ is also some positive scalar constant, and $\eta(t) \in \Re^{4(n-m)+4}$ is given by $\eta = [x^T,\ \tilde{\theta}^T]^T$. Thus, provided that the conditions in Eqs. (27)–(29) and (42) are satisfied, $\dot{V}(t)$ is strictly negative outside the compact set $\Omega_\eta = \{\eta(t) \mid 0 \leq \|\eta(t)\| \leq \sqrt{\gamma/c}\}$. This means that $V(t)$ is decreasing outside the set Ω_η, which results in the following inequality:

$$V(t) \leq V(0) \leq \lambda_\upsilon\|\upsilon(0)\|^2 + 0.5\lambda_{\max}(\Gamma^{-1})\left\|\tilde{\theta}(0)\right\|^2\ \ \forall t \geq 0, \tag{45}$$

where the upper bound on $V(t)$ in inequality (33) is used. From inequalities (45) and (33), one has

$$\|x\|^2 \leq \lambda_\upsilon/\lambda_x\|\upsilon(0)\|^2 + 0.5\lambda_{\max}(\Gamma^{-1})/\lambda_x\left\|\tilde{\theta}(0)\right\|^2. \tag{46}$$

Therefore, a sufficient condition for inequality (42) is given by

$$\alpha_m > 0.5(\zeta_1 + \zeta_3) + 0.5(\zeta_2 + \zeta_4)(\lambda_\upsilon/\lambda_x\|\upsilon(0)\|^2 + 0.5\lambda_{\max}(\Gamma^{-1})/\lambda_x\|\tilde{\theta}(0)\|^2). \tag{47}$$

This means that the region of attraction in Eq. (30) can be made arbitrarily large to include any initial condition by selecting the control gains large enough. Hence, $\|\eta(t)\|$ is SGUUB. By considering the properties of saturation functions, this result implies that $e(t) - z(t), z(t),\ r_1(t),\ r_2(t),\ \tilde{\theta}(t) \in L_\infty$, which results in $e(t) \in L_\infty$. The above discussion means that the tracking errors, state estimation errors, and parameter estimation errors are SGUUB. Therefore, by considering Eqs. (13) and (15), one concludes that $\dot{e}(t),\ \dot{z}(t) \in L_\infty$. As a result, considering Eqs. (6) and (7), the control law in Eq. (17), and Assumption 2, one gets $q(t),\ v(t),\ \hat{v}(t),\ \hat{\theta}(t),\ u_a(t) \in L_\infty$. This completes the proof. □

https://doi.org/10.1017/S0263574714000046 Published online by Cambridge University Press

3.4. Remarks

Remark 1. Considering the definition of $\dot{y}_r(t)$ in Eq. (12) and the observer definition in Eqs. (19) and (20), the signal $\ddot{y}_r = \ddot{y}_d - \Lambda\, s'(\hat{y} - y_d)(\dot{\hat{y}} - \dot{y}_d)$ is available for the computation of $\hat{\rho}(\dot{y}_r,\ \ddot{y}_r)$ in the proposed controller in Eq. (17).

Remark 2. It should be noted that the resulting internal dynamics of the WMR input–output model in Eq. (8) depends on the output choice in Eq. (6). The effectiveness of an inverse dynamic controller, which is designed based on Eq. (8), hinges upon the stability of such internal dynamics. Yun and Yamamoto[34] investigated the stability properties of the internal dynamics of a nonholonomic WMR for the case of look-ahead control method. The look-ahead control takes the coordinates of a reference point in the front of a mobile robot as the output equation. By designing a nonlinear controller, the reference point can follow any desired trajectory. They showed that the internal dynamics is stable when the WMR is commanded to move forward, but it is unstable when it moves backward. Based on the presented stability results on the internal dynamics of WMRs in Yun and Yamamoto[34], the look-ahead control strategy is adopted in this paper to choose suitable output equations. Otherwise, it is necessary to analyze the stability of the resulting internal dynamics for every new set of output equations in Eq. (6) chosen by the designer. The proposed method is applicable to different types of WMRs, including differential, synchro, and Ackermann drive robots by choosing a suitable set of output equations.

Remark 3. In order to make the proposed controller in Eq. (17) and the adaptive law in Eq. (18) independent from velocity measurements, the term $r_1 + r_2$ is substituted by $\hat{r}_1 + \hat{r}_2 := \dot{\hat{y}} - \dot{y}_d + \Lambda\, s(\hat{y} - y_d) + \Lambda\, s(\mathrm{z})$. In fact, if the gains are set large enough, the approximation $r_1 + r_2 = \hat{r}_1 + \hat{r}_2$ is satisfied. The interested reader is referred to Arteaga and Kelly[33] for a similar discussion.

Remark 4. The conditions in Eqs. (27)–(29) in Theorem 1 present sufficient conditions for the stability of the closed-loop system as the result of the conservative Lyapunov-based stability analysis. One may find less restrictive sufficient conditions on control gains in the stability proof.

Remark 5. The controller–observer parameters Λ, K_1, K_2, k_d, Γ, σ, and θ_0 may be tuned to adjust the convergence rate c and the size of ultimate bound γ/c. For example, the following tuning rules can be deduced from the above stability analysis which help the user to properly adjust control parameters: (*i*) considering Eq. (40), the larger values of Λ, K_2, and k_d increase c and decrease the size of the ultimate bound γ/c; (*ii*) smaller values of σ decrease the value of γ and consequently leads to smaller ultimate bound γ/c; (*iii*) the time function $\varepsilon_t(t)$ in saturation-type controller $s(\bullet)$ in Eq. (17) may be tuned to compromise between the final tracking accuracy and smoothness of the control signal. The controller in Eq. (17) may be made smoother by choosing a larger value for $\varepsilon_t(t)$. However, larger value of $\varepsilon_t(t)$ increases the value of $\gamma(t)$ in inequality (44), which may result in a larger ultimate bound γ/c.

4. A Simulation Study

4.1. Control of a nonholonomic differential drive WMR

A differential drive WMR has one of the most popular locomotion systems with nonholonomic constraints in mobile robotics whose planar configuration is shown by Fig. 2. This type of WMR can change its direction by changing the relative angular velocities of its active wheels, which are located on either side of the WMR body. The active wheels are two conventional fixed wheels on a single common axle and are motorized separately. Two passive castor wheels are also placed in the rear and front of the WMR to maintain its equilibrium. According to Fig. 2, the center of mass of the robot is located in $P_C = (x_C, y_C)$. The point $P_0 = (x_O, y_O)$ is the origin of the local coordinate frame that is attached to the robot body and is located at a distance d from P_C. The point $P_L = (x_L, y_L)$ is a virtual reference point on x-axis of the local frame at a distance L (look-ahead distance) of P_O.[4] If the generalized coordinate vector is selected to be $q = [x_O, y_O, \varphi]^T$, one velocity constraint is obtained as $\dot{y}_O \cos\varphi - \dot{x}_O \sin\varphi = 0$. Thus, we define pseudo-velocities of the nonholonomic robot

https://doi.org/10.1017/S0263574714000046 Published online by Cambridge University Press

Table I. Kinematic and dynamic parameters of nonholonomic differential drive WMR and their attributed values for the simulation.

Parameter	Description	Value
r	Radius of driving wheels	0.1 m
$2b$	Distance between two wheels	0.6 m
d	Distance of point P_C from point P_O	0.05 m
L	Distance of point P_O from point P_L	0.15 m
m_c	Mass of platform without driving wheels and rotors of DC motors	10 kg
m_w	Mass of each driving wheel plus the rotor of its motor	0.2 kg
I_c	Moment of inertia of platform without driving wheels and rotors of motors about a vertical axis through P_C	3 kg m^2
I_m	Moment of inertia of each wheel and motor rotor about a wheel diameter	0.006 kg m^2

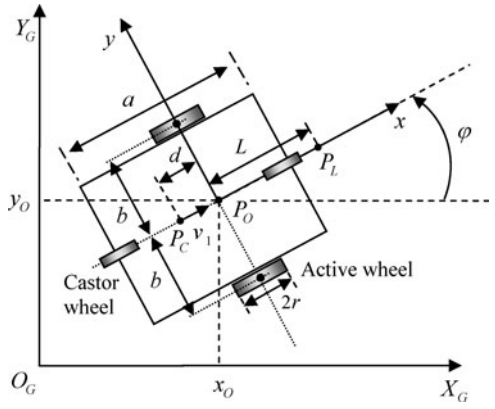

Fig. 2. Planar configuration of a nonholonomic WMR.

as $v(t) = [v_1(t),\ v_2(t)]^T$, in which v_1 and v_2 denote the linear and angular velocities of the robot respectively. According to the notation introduced in Section 2, the following kinematic and dynamic matrices may be obtained[4,20]:

$$S(q) = \begin{bmatrix} \cos\varphi & 0 \\ \sin\varphi & 0 \\ 0 & 1 \end{bmatrix} \quad M_1(q) = \begin{bmatrix} m & 0 \\ 0 & I \end{bmatrix}, \quad C_1(q,\dot{q}) = \begin{bmatrix} 0 & m_c d\dot{\varphi} \\ -m_c d\dot{\varphi} & 0 \end{bmatrix}, \tag{48}$$
$$X_1 = \begin{bmatrix} 1/r & b/r \\ 1/r & -b/r \end{bmatrix}, \quad B_1 = X_1^T, \ D_m = 0, \ G_1(q) = 0,$$

where $m = m_c + 2m_w$ and $I = I_c + 2I_m + m_c d^2 + 2m_w b^2$. Tables I and II show definitions of WMR parameters for simulation. Different sources of uncertainties exist in the WMR model, some of which are listed as follows: (*i*) the uncertain values of the kinematic, dynamic, and actuator parameters of the WMR; (*ii*) the unmodeled dynamics of the passive castor wheels; (*iii*) the wheel slippage, Coulomb and viscous frictions; (*iv*) nonidealities of the mechanical parts of the WMR; (*v*) additive measurement noise; and (*vi*) unwanted bounded disturbances, such as external forces. To follow the controller design procedure which is given in previous sections, the following output variables are chosen to track the desired trajectory based on *look-ahead control* method ($n - m = 2$)[4,18]:

$$y = [h_1(q),\ h_2(q)]^T = [x_O + L\cos\varphi,\ y_O + L\sin\varphi]^T. \tag{49}$$

This choice of output equations is necessary to guarantee the existence of inversion of matrix $J(q)$ in Eq. (7) for the design of the proposed controller. By considering Eqs. (8), (48), and (49) and simple

https://doi.org/10.1017/S0263574714000046 Published online by Cambridge University Press

Table II. Motor parameters and their attributed values for the simulation.

Parameter	Description	Value
r_a	Motor armature resistance	5 Ω
l_a	Motor armature inductance	0.1 Ω-s
k_τ	Motor torque constant	0.2 oz-in/A
k_b	Back EMF constant	0.02 V/rad/s
n	Gear box ratio	48
k_{a1}	Motor constant which depends on motor parameters	1.92
k_{a2}	Motor constant which depends on motor parameters	1.84

numerical computations, one has

$$M_2 = K_{a1}^{-1}\begin{bmatrix} m\cos^2\varphi + I/L^2(1-\cos^2\varphi) & 0.5(m - I/L^2)\sin(2\varphi) \\ 0.5(m - I/L^2)\sin(2\varphi) & I/L^2\cos^2\varphi + m(1-\cos^2\varphi) \end{bmatrix}, \tag{50}$$

$$C_2 = K_{a1}^{-1}\begin{bmatrix} -0.5\dot{\varphi}\sin(2\varphi)(m - I/L^2) & m\dot{\varphi}\cos^2\varphi + I/L^2\dot{\varphi}\sin^2\varphi + m_C d\dot{\varphi}/L \\ -m\dot{\varphi}\sin^2\varphi - I/L^2\dot{\varphi}\cos^2\varphi - m_C d\dot{\varphi}/L & 0.5\dot{\varphi}\sin(2\varphi)(m - I/L^2) \end{bmatrix}. \tag{51}$$

A simple analysis shows that the matrices M_2 and C_2 satisfy the structural properties presented in Section 2.[24]

4.2. Simulation results

This section presents some numerical simulations to illustrate tracking performance, robustness, and power consumption of the proposed controller for a WMR subjected to both parametric and nonparametric uncertainties. All of the simulations are carried out using MATLAB software. Kinematic and dynamic models and actuator dynamics of WMR are considered to simulate a more realistic robot. Gaussian white noise is also added to the output measurements using *randn*(•) function to simulate a localization system. The real values of WMR parameters, depicted in Tables I and II, are chosen to match with a real mobile robot. All simulations are performed based on Euler approximation with a time step of 20 ms. It is assumed that inertia and actuator parameters are unknown. The following model is chosen to simulate nonparametric uncertainties such as friction, unmodeled dynamics, and disturbances:

$$\tau_{d1}(t) = 0.8 I_2 v + 0.5\, I_2 \mathrm{sgn}(v) + [10\sin(0.05\,t),\ \ 10\sin(0.05\,t)]^T. \tag{52}$$

The following desired trajectory is selected to evaluate the controller performance:

$$\begin{aligned} y_d &= [y_{d1}(t),\, y_{d2}(t)]^T, \\ y_{d1}(t) &= x_g + R\sin(c_1\omega_r t) + R\cos(c_2\omega_r t), \\ y_{d2}(t) &= y_g + R\sin(c_2\omega_r t) + R\cos(c_1\omega_r t), \end{aligned} \tag{53}$$

where $(x_g, y_g) = (2.5\,\mathrm{m},\ 5.5\,\mathrm{m})$, $R = 2\,\mathrm{m}$, $\omega_r = 0.05$ rad/s, and $c_1 = 2$ and $c_2 = 1$ are the parameters of the desired trajectory. In this simulation, the following controller parameters achieve a satisfactory tracking performance: $K_1 = 50\ I_2$, $K_2 = 100\ I_2$, $\lambda = 2.2$, $k_d = 10$, $\varepsilon_t(t) = 1$, $\Gamma = \mathrm{diag}[1,\ 1,\ 0.25,\ 1]$, $\sigma = 0.005$, and $\theta_0 = 0$. However, one may take Remark 5 into account to choose control parameters to obtain a more desirable tracking performance. A hyperbolic tangent function is applied as a saturation function to evaluate the proposed controller. The control signals are saturated within $|u_{ai}| \le 24\,V$, $i = 1,\ 2$ to simulate the actuator saturation. The initial postures (the position and orientation) of the WMR are set to $x_O(0) = 15.0\,\mathrm{m}$, $y_O(0) = 12.0\,\mathrm{m}$, and $\varphi(0) = -\pi/6$ rad for this simulation. The other initial conditions are selected as $z(0) = 0$, $\hat{y}(0) = 0$, $\hat{\theta}(0) = [1,\ 0,\ 0,\ 0]^T$. In addition, it is assumed that the WMR is initially at rest. Simulation results, including the WMR

https://doi.org/10.1017/S0263574714000046 Published online by Cambridge University Press

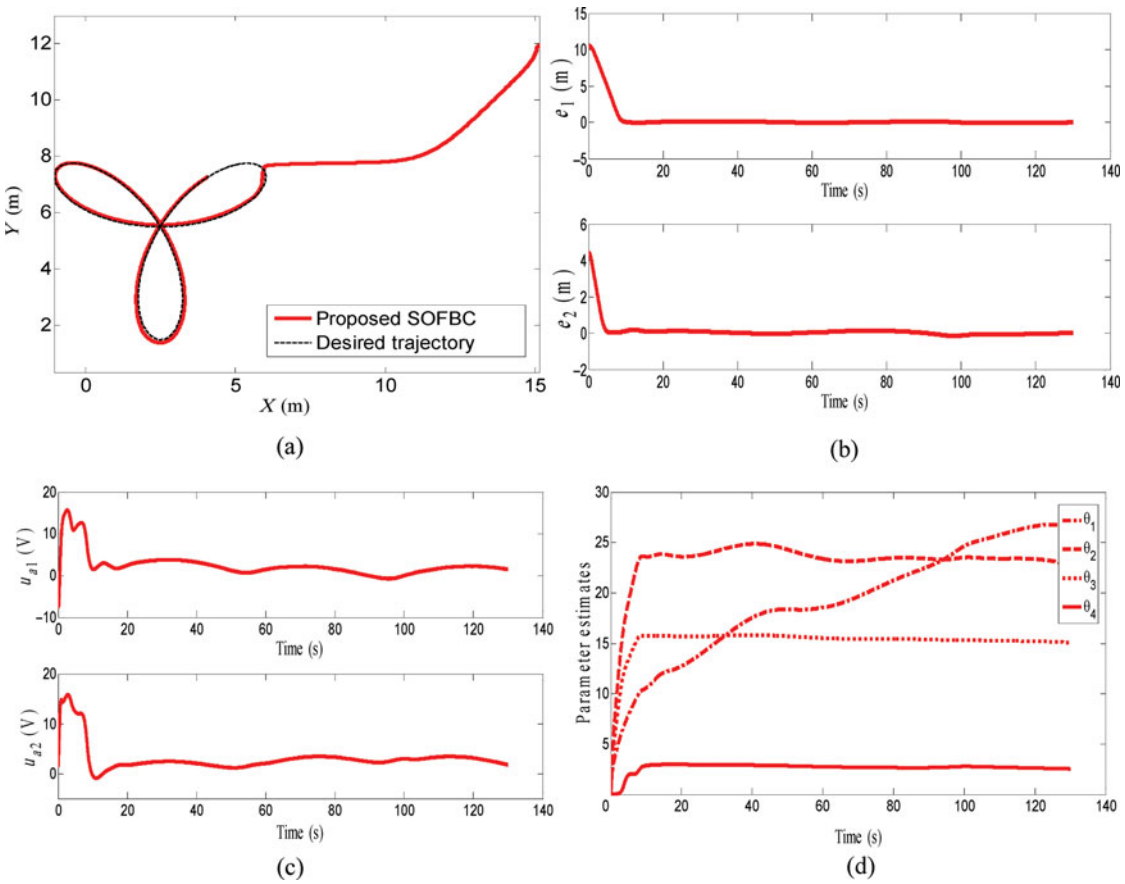

Fig. 3. (Colour online) (a) X–Y plot of the desired trajectory and WMR trajectory for the proposed controller, (b) output tracking errors, (c) the control signals, and (d) the estimated parameters of the upper-bounding functions of uncertain nonlinearities.

trajectories, output tracking errors, control signals, and the estimated parameters of the upper bounding function of uncertain nonlinearities are illustrated in Fig. 3.

As shown in the figure, the proposed SOFBC forces the WMR to track the desired trajectory without actuator saturation. Further simulations show that the proposed SOFBC successfully copes with the trajectory-tracking problem even for large initial tracking errors in the presence of model uncertainties, actuator constraints, and only position measurements. This will comparatively be studied in the next section.

4.3. Comparative studies

4.3.1. Qualitative comparisons. In this section, it is of interest to compare the proposed SOFBC with previously proposed controllers. In order to evaluate the effectiveness of the proposed SOFBC, an OFBC similar to that of Shojaei and Shahri[24] is considered as follows:

$$u_a = B_2^{-1}(q)(-K_1(\dot{y}_o - \dot{y}_r) - K_2(e+z) - (\hat{r}_1 + \hat{r}_2)\hat{\rho}^2/(\hat{\rho}\,\|\,\hat{r}_1 + \hat{r}_2\| + \varepsilon_t(t))), \tag{54}$$

where $\hat{\rho}(\dot{y}_r,\ \ddot{y}_r) = G(\dot{y}_r,\ \ddot{y}_r)\hat{\theta}$, $\hat{\theta}$ is updated by Eq. (18) and the observer definition is given by

$$\dot{\hat{y}} = \dot{\hat{y}}_o + \Lambda z + k_d z, \tag{55}$$

$$\ddot{\hat{y}}_o = \ddot{y}_r + k_d \Lambda z. \tag{56}$$

Scenario 1: The control parameters of the controller in Eq. (54) are chosen as $K_1 = 0.5\ I_2$, $K_2 = 0.5\ I_2$, $\lambda = 0.5$, and $k_d = 10$. The parameters of the adaptive robust control term for both controllers are also set to $\Gamma = 0.1\text{diag}[1,\ 1,\ 0.1,\ 1]$, $\sigma = 0.001$, $\varepsilon_t(t) = 10$, and $\theta_0 = 0$. The

https://doi.org/10.1017/S0263574714000046 Published online by Cambridge University Press

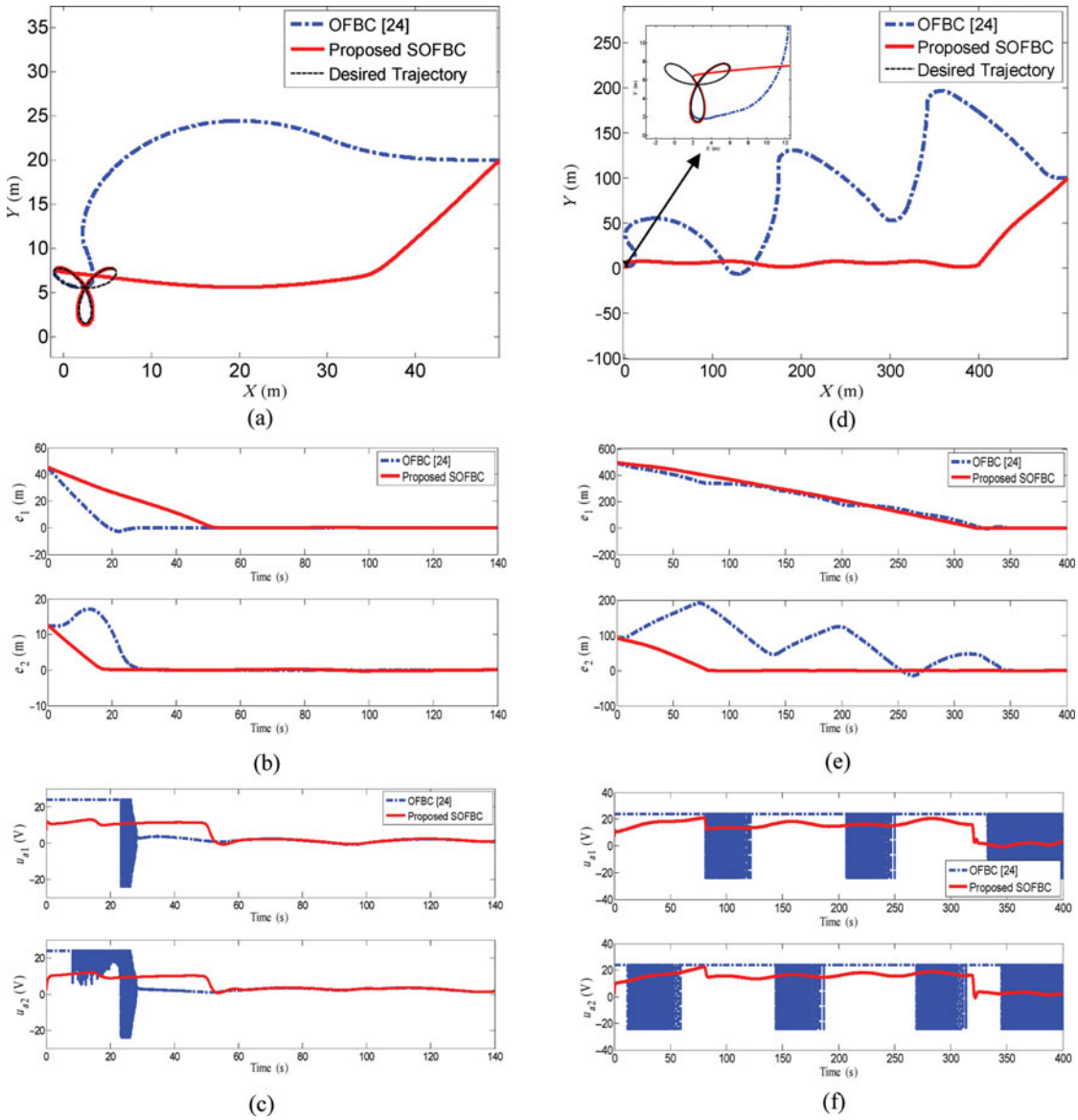

Fig. 4. (Colour online) Comparison of the proposed SOFBC and OFBC of ref. [24] given by Eq. (54). Scenario 1: (a) X–Y plot of the desired trajectory and WMR trajectory for both controllers, (b) output tracking errors, (c) control signals. Scenario 2: (d) X–Y plot for both controllers, (e) output tracking errors, and (f) control signals.

proposed SOFBC gains and other simulation parameters are the same as previous simulation. The initial posture of the WMR are set to $x_O(0) = 50\,\text{m}$, $y_O(0) = 20\,\text{m}$, and $\varphi(0) = -\pi$ rad. The WMR trajectories, output tracking errors, and control signals are illustrated in Figs. 4(a)–(c). As shown in this figure, the proposed controller in Eq. (17) provides a smoother transient response than the controller in Eq. (54). Compared with the proposed controller in Eq. (17), generated signals of the controller in Eq. (54) are saturated during the tracking. This situation is even deteriorated for very large initial tracking errors.

Scenario 2: A very large initial posture, $x_O(0) = 500\,\text{m}$, $y_O(0) = 100\,\text{m}$, $\varphi(0) = -\pi$ rad, is chosen to compare both controllers again. Control gains are selected as scenario 1. The simulation results are provided by Figs. 4(d)–(f). As shown in this figure, the proposed controller in Eq. (17) makes the WMR track smoothly the desired trajectory without actuator saturation. While the controller in Eq. (54) leads to actuator saturation, which, in turn, results in a poor tracking performance for the WMR. In practice, the actuators cannot tolerate such control signals, and the tracking performance is

https://doi.org/10.1017/S0263574714000046 Published online by Cambridge University Press

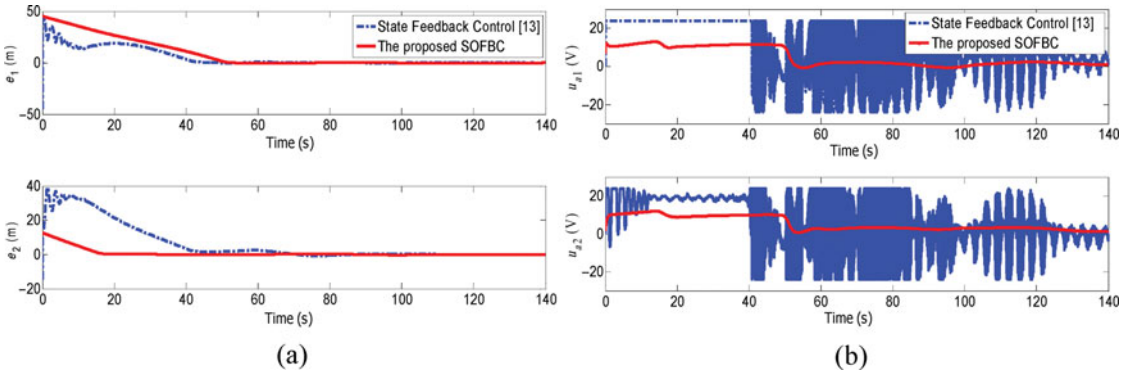

Fig. 5. (Colour online) Comparison of the proposed SOFBC and controller of ref. [13] for scenario 1: (a) position tracking errors, and (b) control signals.

highly degraded. Note that the actuator saturation and the control chattering may be reduced for the controller in Eq. (54) by reducing the control gains, but selection of small gains for the controller in Eq. (54) remarkably degrades the closed-loop performance in comparison with the proposed SOFBC in this paper.

According to the presented comparative studies in refs. [23, 24], the proposed OFBCs in refs. [21, 22, 23] show very poor tracking performances in the presence of nonparametric uncertainties in Eq. (52). As a result, one can definitely infer the superiority of the SOFBC proposed in this paper.

To further investigate the performance of the proposed SOFBC, a traditional adaptive robust backstepping controller is designed based on the ref. [13] for comparison with the proposed SOFBC in Eq. (17). The proposed controller in ref. [13] is designed based on the kinematic controller of ref. [3], which is recommended by many studies according to ref. [13]. The simulation conditions, including robot parameters, desired trajectory, and model uncertainties, are carefully adapted to the presented scenarios in this paper. The details are omitted here due to limited space and the interested reader is referred to ref. [13] for controller equations and parameters. Figure 5 shows the tracking errors and control signals of the proposed SOFBC and the controller in ref. [13] for scenario 1. In Fig. 5, one can see the superiority of the proposed SOFBC in this paper from the viewpoint of transient response and power consumption. The proposed controller of ref. [13] completely fails to follow the desired trajectory in scenario 2, not illustrated here.

4.3.2. Quantitative comparisons. For a fair comparative study of the controllers in quantity, the following performance indexes are defined as in ref. [35]:

- The following root mean square (rms) of the tracking error is used to evaluate the *average tracking performance*:

$$\text{rms}(e_j(t)) = \sqrt{(1/T_f)\int_0^{T_f} |e_j(t)|^2 dt}, \quad j = 1,\ 2, \tag{57}$$

  where T_f denotes the total running time and e_j represents the tracking error for jth output.
- The following rms of control signals is used to evaluate the amount of *control efforts*, which, in turn, is used to measure the amount of control power consumption:

$$\text{rms}(u_{aj}(t)) = \sqrt{(1/T_f)\int_0^{T_f} |u_{aj}(t)|^2 dt}, \quad j = 1,\ 2. \tag{58}$$

- $e_{M,j} = \max_t\{|e_j(t)|\},\ j = 1, 2$, the maximum absolute value of the tracking error, is used to assess the *transient performance* of controllers.
- $e_{f,j} = \max_{T_f - T_L \le t \le T_f}\{|e_j(t)|\},\ j = 1, 2$, the maximum absolute value of the tracking error during the last T_L seconds, is used as an index of measure of *final tracking accuracy* of controllers (in this simulation, $T_L = 5$ s).

https://doi.org/10.1017/S0263574714000046 Published online by Cambridge University Press

Table III. The quantitative comparative study of controllers in refs. [13, 24] and the proposed SOFBC of this paper.

	Output feedback control[24]		State feedback control[13]		Proposed SOFBC	
Performance index	Scenario 1	Scenario 2	Scenario 1	Scenario 2	Scenario 1	Scenario 2
rms($e_1(t)$) (m)	65.6	1813.3	85.25	2217	111	1935.5
rms($e_2(t)$) (m)	39.9	666.2	72.15	473.5	17.8	189.1
rms($u_{a1}(t)$) (V)	10,946	5×10^{10}	568	3×10^{6}	48	104.5
rms($u_{a2}(t)$) (V)	4694	4.8×10^{10}	142	3×10^{6}	45.8	103.1
rms($u_{as1}(t)$) (V)	74.9	169.7	127.2	169.7	48	104.5
rms($u_{as2}(t)$) (V)	72.8	169.7	113.4	169.7	45.8	103.1
$e_{M,1}$ (m)	45.35	495.3	45.5	495	45.3	495.3
$e_{M,2}$ (m)	17.08	191.4	24.8	93	12.50	92.5
$e_{f,1}$ (m)	0.06	0.09	0.08	126.9	0.07	0.06
$e_{f,2}$ (m)	0.07	0.11	0.08	7	0.09	0.08
Overall performance	Efficient	Efficient	Efficient	Inefficient	Efficient	Efficient
Power consumption	Very high	Inefficient	High	Inefficient	Low	Low

Table III demonstrates the numerical values of the above performance indexes, which compare the controllers from the viewpoint of overall performance and power consumption. It can be seen that the amount of control efforts, i.e. rms($u_{aj}(t)$), and saturated control, i.e. rms($u_{asj}(t)$), for the proposed SOFBC is remarkably smaller than that of the proposed controllers in refs. [13, 24]. The proposed SOFBC also shows a better transient performance compared with other controllers. However, the controllers try to outperform in the average tracking performance and final tracking accuracy. The qualifications of all the controllers are depicted in the last two rows of the table. A significant conclusion from Table III is that the proposed SOFBC is more effective than the previous works for large initial tracking errors considering the actuator saturation problem.

5. Conclusions

In this paper the trajectory tracking control problem of uncertain nonholonomic mobile robotic systems has been addressed. Based on the second-order input–output model of nonholonomic systems, a saturated OFBC is designed such that it makes the tracking errors SGUUB in the presence of actuator saturation, structured and unstructured uncertainties, and without measurement of velocity signals. The main feature of the proposed controller is that it mitigates the actuator saturation, which, in turn, improves the transient performance for large initial tracking errors in the trajectory-tracking problem. The Lyapunov-based stability analysis is utilized to show semi-global uniform ultimate boundedness of tracking and sate estimation errors. The proposed controller has been applied to trajectory tracking control of a differentially driven nonholonomic WMR. A comparative simulation study has been presented which shows that the proposed controller is more efficient than previous works for the sake of actuator saturation and better transient response. In the subsequent researches, the experimental evaluation of the proposed SOFBC on a real WMR is taken into account to support the presented theories and simulation results.

Acknowledgements

The author would like to thank associate editor and anonymous reviewers for their valuable comments for improving the original manuscript.

References

1. R. W. Brockett, "Asymptotic Stability and Fedback Stabilization," **In**: *Differential Geometric Control Theory* (R. W. Brockett, R.S. Milman and H. J. Sussman, eds.) (Birkhauser, Boston, MA, 1983) pp. 181–191.
2. G. Campion, B. d'Andrea-Novel and G. Bastin, "Modeling and State Feedback Control of Nonholonomic Mechanical Systems," *Proceedings of IEEE International Conferenceon on Decision and Control* (1991) pp. 1184–1189.

https://doi.org/10.1017/S0263574714000046 Published online by Cambridge University Press

3. Y. Kanayama, Y. Kimura, F. Miyazaki and T. Nogushi, "A Stable Tracking Control Method for an Autonomous Mobile Robot," *Proceedings of IEEE International Conference on Robotics and Automation* (1990) pp. 384–389.
4. N. Sarkar, X. Yun and V. Kumar, "Control of mechanical systems with rolling constraint: Application to dynamic control of mobile robots," *Int. J. Robot. Res.* **13**(1), 55–69 (1994).
5. I. Kolmanovsky and H. McClamroch, "Developments in nonholonomic control problems," *Control Syst. Mag. (IEEE)* **15**(6), 20–36 (Dec. 1995).
6. Z-P Jiang and H. Nijmeijer, "A recursive technique for tracking control of dynamic nonholonomic systems in chained form," *IEEE Trans. Autom. Control* **34**(32), 265–279 (1999).
7. T. Fukao, H. Nakagawa and N. Adachi "Trajectory tracking control of a nonholonomic mobile robot," *IEEE Trans. Robot. Autom.* **16**(5), 609–615 (2000).
8. W. Dong and W. L Xu, "Adaptive tracking control of uncertain nonholonomic dynamic system," *IEEE Tans. Autom. Control* **46**(3), 450–454 (2001).
9. M. Oya, C.-Y. Su and R. Katoh, "Robust adaptive motion/force tracking control of uncertain nonholonomic mechanical systems," *IEEE Trans. Robot. Autom.* **19**(1), 175–181 (2003).
10. W. E. Dixon, E. Zergerglu and D. M. Dawson, "Global robust output feedback tracking control of robot manipulators," *Robotica* **22**, 351–357 (2004).
11. W. E. Dixon, "Adaptive regulation of amplitude limited robot manipulators with uncertain kinematics and dynamics," *IEEE Trans. Autom. Control* **52**(3), 488–493 (2007).
12. Z. G. Hou, A. M. Zou, L. Cheng and M. Tan, "Adaptive control of an electrically driven nonholonomic mobile robot via backstepping and fuzzy approach," *IEEE Trans. Control Syst. Technol.* **17**(4), 803–815 (2009).
13. C.-Y. Chen, T.-H. S. Li, Y.-C. Yeh and C.-C. Chang, "Design and implementation of an adaptive sliding-mode dynamic controller for wheeled mobile robots," *Mechatronics* **19**, 156–166 (2009).
14. B. S. Park, S. J. Yoo, J. B. Park and Y. H. Choi, "A simple adaptive control approach for trajectory tracking of electrically driven nonholonomic mobile robots," *IEEE Trans. Control Syst. Technol.* **18**(5), 1199–1206 (2010).
15. D. Chwa, "Tracking control of differential-drive wheeled mobile robots using a backstepping-like feedback linearization," *IEEE Trans. Syst. Man Cybern.* **40**(6), 1285–1295 (2010).
16. S. J. Yoo, "Adaptive tracking control for a class of wheeled mobile robots with unknown skidding and slipping," *IET Control Theory Appl.* **4**(10), 2109–2119 (2010).
17. H. C. Cho, M. S. Fadali, K. S. Lee and N. H. Kim, "Adaptive position and trajectory control of autonomous mobile robot systems with random friction," *IET Control Theory Appl.* **4**(12), 2733–2742 (2010).
18. K. Shojaei, A. Mohammad Shahri, A. Tarakameh and B. Tabibian, "Adaptive trajectory tracking control of a differential drive wheeled mobile robot," *Robotica* **29**, 391–402 (2010).
19. K. Shojaei, A. Mohammad Shahri and A. Tarakameh, "Adaptive feedback linearizing control of nonholonomic wheeled mobile robots in presence of parametric and nonparametric uncertainties," *Robot. Comput. Integr. Manuf.* **27**, 194–204 (2011).
20. K. Shojaei and A. M. Shahri, "Adaptive robust time-varying control of uncertain nonholonomic robotic systems," *IET Control Theory Appl.* **6**(1), 90–102 (2012).
21. K. D. Do, Z-P. Jiang and J. Pan "A global output-feedback controller for simultaneous tracking and stabilization of unicycle-type mobile robots," *IEEE Trans. Robot. Autom.* **20**(3), 589–594 (2004).
22. K. D. Do and J. Pan, "Global output-feedback path tracking of unicycle-type mobile robots," *Robot. Comput. Integ. Manuf.* **22**, 166–179 (2006).
23. B. S. Park, S. J. Yoo, J. B. Park and Y. H. Coi, "Adaptive ouput-feedback control for trajectory tracking of eletcrically driven non-holonomic mobile robots," *IET Control Theory Appl.* **5**(6), 830–838 (2011).
24. K. Shojaei and A. M. Shahri, "Output feedback tracking control of uncertain non-holonomic wheeled mobile robots: A dynamic surface control approach," *IET Control Theory Appl.* **6**(2), 216–228 (2012).
25. E.-H. Guechi, J. Lauber, M. Dambrine and M. Defoort, "Output feedback controller deign of a unicycle-type mobile robot with delayed measurements," *IET Control Theory Appl.* **6**(5), 726–733 (2012).
26. J. Huang, C. Wen, W. Wang and Z.-P. Jiang, "Adaptive stabilization and tracking control of a nonholonomic mobile robot with input saturation and disturbance," *Syst. Control Lett.* **62**, 234–241 (2013).
27. Y. Su and C. Zheng, "Global Asymptotic Stabilization and Tracking of Wheeled Mobile Robots with Actuator Saturation," *Proceedings of the 2010 IEEE International Conference on Robotics and Biomimetics* (2010) pp. 345–350.
28. F. L. Lewis, C. T. Abdallah and D. M. Dawson, *Control of Robot Manipulators* (MacMillan, New York, NY, 1993).
29. F. N. Martins, W. C. Celeste, R. Carelli, M. S-Filho and T. F. B-Filho "An adaptive dynamic controller for autonomous mobile robot trajectory tracking," *J. Control Eng. Pract.* **16**, 1354–1363 (2008).
30. E. Aguinaga-Ruiz, A. Zavala-Rio, V. Santibanez and F. Reyes "Global trajectory tracking through static feedback for robot manipulators with bounded inputs," *IEEE Trans. Control Syst. Technol.* **17**(4), 934–944 (2009).
31. B. Yao, "Adaptive Robust Control of Nonlinear Systems with Application to Control of Mechanical Systems," *Ph.D. thesis*, University of California at Berkeley, 1996.
32. P. A. Ioannou and J. Sun, *Robust Adaptive Control* (Prentice-Hall, Englewood Cliffs, NJ, 1996).

https://doi.org/10.1017/S0263574714000046 Published online by Cambridge University Press

33. M. A. Arteaga and R. Kelly "Robot control without velocity measurements: New theory and experimental results," *IEEE Trans. Robot. Autom.* **20**(2), 297–308 (2004).
34. X. Yun and Y. Yamamoto, "Stability analysis of the internal dynamics of a wheeled mobile robot," *J. Robot. Syst*. **14**(10), 697–709 (1997).
35. L. Xu and B. Yao "Output feedback adaptive robust precision motion control of linear motors," *Automatica* **37**, 1029–1039 (2001).

https://doi.org/10.1017/S0263574714000046 Published online by Cambridge University Press